FEMS Microbiology Ecology, 96, 2020, fiaa121

doi: 10.1093/femsec/fiaa121
Advance Access Publication Date: 18 June 2020
Research Article

RESEARCH ARTICLE

Cascading effects in freshwater microbial food webs by predatory Cercozoa, Katablepharidacea and ciliates feeding on aplastidic bacterivorous cryptophytes

Karel Šimek[1,2,*,§], Vesna Grujčić[1,†], Indranil Mukherjee[1], Vojtěch Kasalický[1,#], Jiří Nedoma[1], Thomas Posch[3], Maliheh Mehrshad[1,‡] and Michaela M. Salcher[1,Δ]

[1]Biology Centre CAS, Institute of Hydrobiology, Na Sádkách 7, 370 05 České Budějovice, Czech Republic, [2]University of South Bohemia, Faculty of Science, Branišovská 31, 370 05 České Budějovice, Czech Republic and [3]Limnological Station, Department of Plant and Microbial Biology, University of Zurich, 8802 Kilchberg, Switzerland

[*]**Corresponding author:** Biology Centre CAS, Institute of Hydrobiology, Na Sádkách 7, CZ-37005 České Budějovice, Czech Republic. Tel: +420 387775873; Fax: +420 385310248; E-mail: ksimek@hbu.cas.cz

One sentence summary: Presented are experimentally induced cascading effects from bacteria to bacterivorous flagellates, predatory flagellates and ciliates in different plankton size fractions, modulated by prey-food characteristics and feeding modes of predominating protists.

Editor: Martin W. Hahn

[†]Current address: Science for Life laboratory, School of engineering sciences in Chemistry, Biotechnology and Health, Department of Gene Technology, KTH Royal institute of Technology, SE-17121, Stockholm, Sweden.
[‡]Current address: Department of Ecology and Genetics, Limnology and Science for Life Laboratory, Uppsala University, Norbyvägen 18D, 752 36 Uppsala, Sweden.
[§]Karel Šimek, http://orcid.org/0000-0002-7058-9063
[#]Vojtěch Kasalický, http://orcid.org/0000-0002-9132-8321
[Δ]Michaela M. Salcher, https://orcid.org/0000-0003-1063-6523

ABSTRACT

Heterotrophic nanoflagellates (HNF) are considered as major planktonic bacterivores, however, larger HNF taxa can also be important predators of eukaryotes. To examine this trophic cascading, natural protistan communities from a freshwater reservoir were released from grazing pressure by zooplankton via filtration through 10- and 5-μm filters, yielding microbial food webs of different complexity. Protistan growth was stimulated by amendments of five *Limnohabitans* strains, thus yielding five prey-specific treatments distinctly modulating protistan communities in 10- versus 5-μm fractions. HNF dynamics was tracked by applying five eukaryotic fluorescence *in situ* hybridization probes covering 55–90% of total flagellates. During the first experimental part, mainly small bacterivorous Cryptophyceae prevailed, with significantly higher abundances in 5-μm treatments. Larger predatory flagellates affiliating with Katablepharidacea and one Cercozoan lineage (increasing to up to 28% of total HNF) proliferated towards the experimental endpoint, having obviously small

Received: 27 April 2020; **Accepted:** 17 June 2020

phagocytized HNF in their food vacuoles. These predatory flagellates reached higher abundances in 10-μm treatments, where small ciliate predators and flagellate hunters also (*Urotricha* spp., *Balanion planctonicum*) dominated the ciliate assemblage. Overall, our study reports pronounced cascading effects from bacteria to bacterivorous HNF, predatory HNF and ciliates in highly treatment-specific fashions, defined by both prey-food characteristics and feeding modes of predominating protists.

Keywords: freshwater microbial food webs; bacterivorous and predatory flagellates; Cryptophyceae; Katablepharidacea; Cercozoa; ciliates

INTRODUCTION

Heterotrophic nanoflagellates (HNF) represent an extremely diverse polyphyletic group of mostly uncultured representatives belonging to a heterogeneous functional guild. The small HNF are considered as key bacterivores in pelagic systems (Berninger, Finlay and Kuuppo-Leinikki 1991; Pernthaler 2005), whereas the larger ones are omnivorous, or likely predators of small bacterivorous flagellates (Arndt *et al.* 2000 and references therein, Piwosz and Pernthaler 2010). However, the term 'omnivorous protists' is still not as clearly defined. This topic gets even more complex in view of current discussions about adequate terminology describing feeding modes of planktonic protists in general (Kiørboe 2011; Weisse 2017). A strict categorization of protistan species as 'algivores' and 'predators' may be valid only for a few distinct taxa, however, this terminology probably does not reflect the breadth of ingested food particles for the majority of protistan grazers (Weisse *et al.* 2016). In our study, we use the term omnivory as a synonym for a flagellate feeding mode where both prokaryotic and eukaryotic food items are ingested.

Apart from the bacterivory mode, which has frequently been studied using surrogates of bacterial prey in various planktonic systems (e.g. Sherr *et al.* 1987; Boenigk and Arndt 2002; Unrein *et al.* 2014; Beisner, Grossart and Gasol 2019), considerably less is known about other feeding modes of larger planktonic HNF (Arndt *et al.* 2000; Domaizon *et al.* 2003; Jeuck and Arndt 2013). The importance of omnivorous or predatory flagellates has rarely been studied under *in situ* conditions, except for their role as algivores, which can be detected via the chlorophyll autofluorescence of ingested prey. Thus, assigning a functional role to these understudied flagellates remains a critical issue.

Two major problems severely constrain progress in studies of flagellate ecology: lack of morphological features allowing for reliable taxonomic identification of larger, supposedly predatory HNF using microscopy (Jeuck and Arndt 2013; Adl *et al.* 2019) and the very limited ability to visualize and characterize the ingested prey of natural flagellate communities if prey organisms do not contain recognizable organelles such as chloroplasts. Consequently, we miss information on the feeding modes of larger HNF (mostly 5–15 μm in size), which may act as an efficient intermediate trophic link in the carbon flow from small bacterivorous HNF to omnivorous or carnivorous ciliates (Arndt *et al.* 2000; Posch *et al.* 2015).

Currently at least some of these limitations can be overcome with the increasing use of amplicon or metagenomic sequencing. For instance, 18S rRNA gene sequences of natural eukaryotic communities can be used for designing novel eukaryotic fluorescence *in situ* hybridization (FISH)-probes, targeting the major players in a given aquatic environment (e.g. Massana *et al.* 2009; Grujčić *et al.* 2018, Piwosz 2019). Thus, taxa with otherwise poor morphological distinguishability can be identified by a strong fluorescence signal and prevailing food items in their food vacuoles can be examined. The double-hybridization technique provides even higher resolution by allowing simultaneous phylogenetic identification of both predator and prey (Grujčić *et al.* 2018). These cumbersome single-cell approaches have recently revealed novel findings on the importance of various flagellate taxa in marine and freshwater pelagic food webs. For instance, tiny flagellated stramenopiles from the MAST-1 and MAST-4 lineages have been identified as important bacterivores in marine systems (Massana *et al.* 2009). Likewise, small aplastidic representatives of cryptophytes (mostly known as chloroplast-bearing autotrophs) and therein the Cry1 lineage can be the core bacterivores with high cell-specific bacterial uptake rates in freshwater pelagic environments (Grujčić *et al.* 2018, Mehrshad and coauthors, unpublished data).

In addition, specific experimental setups were designed with the aim of minimizing the manipulation-induced disturbances of natural microbial communities that yield considerable enrichments of protistan bacterivores (Šimek et al. 2001, 2013). For instance, simplified microbial food webs, that excluded zooplankton grazing pressure on protists by <5 μm size fractionation of natural plankton, amended with bacteria, were dominated by rapidly growing small bacterivorous HNF (Grujčić *et al.* 2018; Šimek et al. 2013, 2018). However, after 2–3 days of incubation, when bacterial prey became depleted, abundances of small HNF dropped dramatically. Concomitantly, we observed a rapid development of larger HNF (6–12 μm, Šimek *et al.* 2018), such as katablepharids (Grujčić *et al.* 2018), that were present in low proportions in the original samples. They had only limited or no uptake of bacteria, suggesting their important role as omnivores or predators preying on eukaryotes mainly in the size fraction of 4–10 μm (Clay and Kugrens 1999; Ok *et al.* 2018).

To test this trophic cascading, natural protistan communities from the freshwater Římov reservoir (Czech Republic) were released from grazing pressure imposed by larger zooplankton via filtration through 10- and 5-μm pore-size filters. This workflow yielded microbial food webs of different complexity, with supposedly higher numbers of larger protists such as predatory flagellates and small ciliates in the 10-μm fraction. Protistan growth in both size fractions was stimulated by additions of five different bacterial strains of the genus *Limnohabitans* isolated from the same environment. These ten prey-specific treatments (five different strains added to two different size fractions) were assumed to distinctly modulate protistan predator communities in 10- versus 5-μm fractions. To track HNF community dynamics, we applied catalyzed reporter deposition fluorescence *in situ* hybridization (CARD-FISH) with eukaryotic probes targeting the dominant HNF populations in the treatments. Ciliate assemblages were analyzed by means of classical staining procedures (Posch *et al.* 2015). The following hypotheses were tested in these experimental manipulations. (i) While small HNF are generally considered as major planktonic bacterivores in freshwaters, larger taxa have comparable growth potential and are important predators of small, primarily bacterivorous HNF. (ii) Releasing HNF from top-down control by zooplankton

in 10-μm treatments will result in enhanced proportions of larger predatory flagellate taxa. (iii) Bacterial amendments of natural plankton in 10-μm treatments will induce profound peaks of primarily bacterivorous ciliate taxa. In the light of our results, the first and second hypotheses were approved, while the third one was rejected.

MATERIAL AND METHODS

Experimental design

Our experimental approach allowed for the detection of changes in both HNF and ciliate abundance and their community composition in two different size fractions of natural plankton that yielded two types of simplified microbial food webs (for details see Fig. 1). Plankton samples were collected from a depth of 0.5 m in the meso-eutrophic Římov reservoir, Czech Republic (48°50′46.90′N, 14°29′15.50′E, for more details see Šimek *et al.* 2001) on 26 August 2013 (water temperature 19°C, Chlorophyll-*a* concentration 6.1 μg l^{-1}). Water was gravity filtered through 10-μm pore-size filters to release the protistan community from grazing pressure by zooplankton and larger ciliates and, for the second set-up, through 5-μm pore-size filters to release the flagellate community from grazing pressure by zooplankton, small ciliates and larger predatory flagellates. Notably, the pre-screened water samples contained almost no small algae, as the summer phytoplankton of the reservoir was dominated by large algal cells (>10 μm) and cyanobacterial colonies. The 5-μm treatment thus represented a simplified prokaryote–HNF food chain supposedly dominated by small, primarily bacterivorous flagellates (Grujčić, Kasalický and Šimek 2015; Šimek et al. 2013, 2018). The 10-μm treatment represented a simplified prokaryote–HNF–small ciliate food chain supposedly dominated by small bacterivorous flagellates, larger predatory flagellates and small, primarily bacterivorous ciliates (Fig. 1).

The filtered samples were preincubated at 18°C for 4 h to allow microbes to recover from the handling shock (Havskum and Riemann 1996). The initial bacterial abundance was identical in both the 5- and 10-μm treatments (AVG ± SD, 4.01 ± 0.12 × 10^6 cells ml^{-1}), while the initial HNF abundance was slightly but insignificantly (*t*-test, $P > 0.05$) higher in 10- compared with 5-μm treatments, 2.24 ± 0.12 × 10^3 cells ml^{-1} compared with 2.14 ± 0.13 × 10^3 cells ml^{-1} (AVG ± SD), respectively. Our experimental set-up yielded 12 different triplicate treatments (1-liter sample volume, Fig. 1), with six treatments each representing the 5- and 10-μm size fractions; one treatment served as control while the others were amended with different bacterial prey (Supplementary Table S1, see online supplementary material). All bacterial strains were isolated from the Římov reservoir and are affiliated to the genus *Limnohabitans*, more specifically to the LimB (Rim11) and LimC lineages (II-D5, II-B4, Rim28, and Rim47, for details see Kasalický *et al.* 2013). The strains II-B4, Rim11 and Rim28 are short rods or cocci with almost identical mean cell volume (MCV, 0.052–0.056 μm^3), Rim47 are cocci of slightly larger MCV (0.080 μm^3), while II-D5 are larger rods (MCV, 0.162 μm^3, see Supplementary Table S1).

The bacterial strains were pre-grown in nutrient-rich liquid medium (3 g l^{-1} NSY, Hahn *et al.* 2004), pelleted by centrifugation, washed and re-suspended in 0.2-μm filtered and sterilized water from the Římov reservoir as described in Grujčić *et al.* (2018). Treatments were separately amended with bacteria added at ∼3–8 times higher amount than the natural bacterial standing stock. Since the bacteria differed in cell size (Supplementary Table S1), the additions of the strains were set to yield approximately the same initial biovolumes for all experimental treatments (referred to as D5-II, B4-II, Rim11, Rim28 and Rim47 throughout the text, see Fig. 1). Bottles containing only natural bacteria and protists, present in the original samples after filtration through 5- and 10-μm filters, served as controls. All triplicate treatments were kept at 18°C in the dark, as the vast majority of protistan grazers were heterotrophic flagellates. Subsamples for quantification of HNF and ciliates (present only in 10-μm treatments) and for bacterial abundances and biovolumes were taken in a laminar flow hood at 12–24 h intervals. Additionally, samples for CARD-FISH analyses were taken at 0, 40 and 66 h, fixed with formaldehyde (2% final concentration) and collected on 1-μm pore-size filters (Grujčić *et al.* 2018).

Enumeration of microbes and calculation of protistan growth parameters

Samples from all triplicate treatments (15–20 ml) were fixed with formaldehyde (2% final concentration) and used for the enumeration of bacteria (0.5–2 ml subsamples) and protists (5–15 ml subsamples) on 0.2 and 1-μm pore-sized filters (Osmonics, Inc., Livermore, CA), respectively. All samples were stained with DAPI (4′,6-diamidino-2-phenylindole, final concentration of 1 μg ml^{-1}) and microbes were counted via epifluorescence microscopy (Olympus BX53; Optical, Tokyo, Japan). Bacterial and flagellate biovolumes were measured using a semiautomatic image analysis system (NIS-Elements 3.0, Laboratory Imaging, Prague, Czechia) as detailed in Šimek *et al.* (2013) and Grujčić, Kasalický and Šimek (2015). The treatment-specific increases in HNF cell numbers were used to calculate maximum HNF growth rates, doubling times (DT) and length of lag phases as described in Šimek *et al.* (2018). Estimates of growth gross efficiency (GGE) of HNF (as % of cell volume) were calculated as the ratio between added bacterial biovolume and net HNF biovolume yields in the treatment (thus representing volumetric GGE, Šimek *et al.* 2018).

Ciliate abundance and assemblage composition

Ciliate abundances and assemblage structure (present only in 10 μm treatments) were evaluated in triplicates by combining epifluorescence microscopy of DAPI-stained samples and quantitative protargol staining (Posch *et al.* 2015 and references therein). For protargol preparations, 10–25 ml of samples fixed with Lugol's solution and postfixed with Bouin's fluid were filtered on 0.8-μm pore-size Nitrocellulose filters (Sartorius). We identified and counted at least 150–200 individuals per sample. For more details on the above approaches see Posch *et al.* (2015) and Šimek *et al.* (2019). Because protargol staining was applied in parallel with fluorescence microscopy for ciliates, we determined most of the ciliates to the genus level and, if possible, to species level. Numbers of ciliates were assessed via direct counting of DAPI-stained cells in samples filtered on 1-μm pore-sized filters (Osmonics). To identify ciliates in fluorescence microscopy we used additional criteria, such as ciliate cell size, the position and size of nuclei, and prey characteristics (Šimek *et al.* 2019). Between 3 and 11% of the ciliates, however, could not be identified. We based our identifications on the publications of Foissner and Berger (1996) and Foissner, Berger and Schaumburg (1999).

Probe design and CARD-FISH analyses of flagellate assemblages

Already published oligonucleotide probes targeting abundant freshwater protistan lineages were assessed for coverage and specificity, using the guide tree of SILVA_138_SSURef _NR99 in

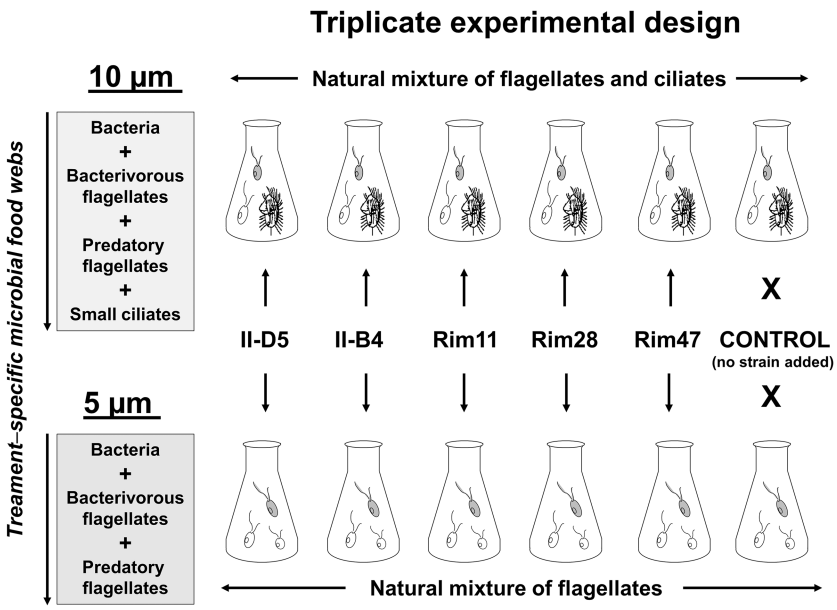

Figure 1. Experimental design: natural microbial communities in 5-µm filtered (presumably dominated by bacterivorous HNF) and 10-µm filtered (containing bacterivorous HNF, predatory HNF and small ciliates) water samples from the Římov reservoir were amended with different bacterial strains from the genus *Limnohabitans* (II-D5, II-B4, Rim11, Rim28, and Rim47) as a major protistan food source. The bacterial strains were added in concentrations compenzating for their cell biovolumes (for details of the bacterial strains see Supplementary Table S1) to yield 3–8-fold of natural bacterial standing stock present in the non-amended 5- and 10-µm filtrates used as controls (Fig. 3). Subsamples were collected at 12–24 h intervals; for more details see Material and Methods.

ARB (Ludwig *et al.* 2004; Quast *et al.* 2013). Additionally, bootstrapped maximum likelihood trees of eukaryotic 18S rRNA genes (GTR-GAMMA model, 100 bootstraps; Stamatakis 2014) were constructed for specific lineages (Fig. 2). The general probe Crypto B that targets 74.3% of all Cryptophyceae excluding Katablepharidacea (Metfies and Medlin 2007) had only one outgroup hit (GU647185, an uncultured freshwater eukaryote, *Ceratium* sp.), while the general probe for Kinetoplastea (Kin516, Bochdansky and Huang 2010) had a very high coverage (96.2%), but also a high number of outgroup hits affiliated to a broad range of microbes (342 outgroup hits: 1 Crenarchaeota, 3 Diplonemea, 258 Amorphae from diverse groups, 7 Spermatophyta, 73 SAR from diverse groups; Fig. 2, Table 1). Nevertheless, we decided to use this probe because of the uniform morphological features of the target group Kinetoplastea, i.e. the presence of both a DNA-containing nucleus and a kinetoplast in DAPI-stained cells that can be easily recognized via epifluorescence microscopy (Mukherjee, Hodoki and Nakano 2015). Probe Cry1–652 targets all 18S rRNA gene sequences of lineage Cry1, and probe Kat-1452 almost all sequences of a freshwater lineage of Katablepharidacea (Grujčić *et al.* 2018; Fig. 2, Table 1). Both probes target no outgroup hits. A specific probe targeting one sequence of Cercozoa affiliated with Novel Clade 7 (AY620288, originating from a freshwater pond; Bass and Cavalier-Smith 2004) was designed because of high similarities to 18S rRNA gene amplicons gained in a previous study (OTU#14 in Grujčić *et al.* 2018). Probe Cerc-193 was designed with the tools probe design and probe test in ARB (Ludwig *et al.* 2004), checked *in silico* for specificity and binding properties (Yilmaz *et al.* 2011; Quast *et al.* 2013) and tested with different formamide concentrations in the hybridization buffer until highest stringency was achieved at 55% (Table 1). We also applied a FISH-probe targeting Haptophyta (PRYM02, Simon *et al.* 2000), but did not detect any stained cells in our samples.

CARD-FISH for flagellates was applied following the detailed protocol described in Piwosz and Pernthaler (2010). CARD-FISH preparations were analyzed by epifluorescence microscopy at 1000 × magnification. The flagellate lineage-specific MCV was calculated based on measurements of the width and length of hybridized cells using an image analysis system (NIS-Elements 3.0), assuming a prolate spheroid cell shape (Šimek *et al.* 2013). Combining CARD-FISH for flagellates with the CARD-FISH protocol for bacteria (Sekar *et al.* 2003) allowed the examination of HNF food vacuoles for ingested bacteria (Jezbera, Horňák and Šimek 2005). The bacterial probe R-BT065 targeting the genus *Limnohabitans* was used to visualize the presence of ingested bacterial prey in food vacuoles (Šimek *et al.* 2013) of different flagellate phylotypes using a double-hybridization protocol (Grujčić *et al.* 2018).

Statistical analysis

Statistically significant differences in growth parameters (growth rate, lag, GGE) between strains and size fractions were determined using two-way ANOVA with Tukey's and Sidak's multiple comparisons post-tests. Differences in bacterial abundances between different size fractions at different times were determined with unpaired *t*-test with Welch's correction. For an objective estimate of the time lag in decrease in bacterial numbers between 5- and 10-µm filtered variants, we first estimated for each variant the incubation time at which half of the decrease occurred (T_{50}) and then calculated their difference. T_{50} values were estimated by fitting the data with a four-parameter logistic model with variable slope using the following equation

$$BacNum = Bottom + (Top - Bottom)/(1 + exp((T_{50} - t) \times Slope)), \quad (1)$$

where *t* is incubation time, *BacNum* is bacterial abundance, *Top*, *Bottom* and *Slope* are upper and lower plateaus and slope of the data, respectively. The data obeyed the model extremely well (r^2 values of 0.988–0.999). Statistical significances of the differences

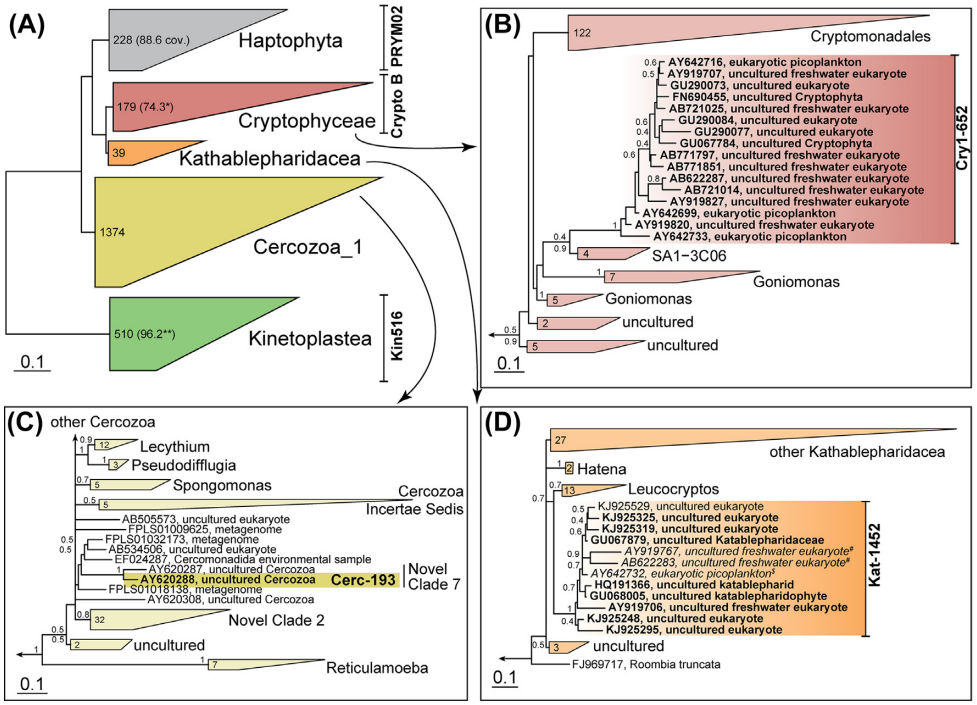

Figure 2. Targets of oligonucleotide probes used for CARD-FISH. (**A**) Extract of the maximum parsimony guide tree of SILVA_138_SSURef_NR99 with branches targeted by general eukaryotic probes PRYM02 (Haptophyta), Crypto B (Cryptophyceae_1) and Kin516 (Kinetoplastea). Values inside the collapsed branches give total numbers of sequences and coverages (%) for each probe. ∗Outgroup hit of probe Crypto B (GU647185, uncultured freshwater eukaryote, *Ceratium*); ∗∗342 outgroup hits of probe Kin516 (1 Crenarchaeota, 3 Diplonemea, 258 Amorphae from diverse groups, 7 Spermatophyta, 73 Stramenopiles, Alveolata, or Rhizaria from diverse groups). (**B–D**) Bootstrapped maximum likelihood trees of eukaryotic 18S rRNA genes with marked target hits of specific probes in bold. Only bootstrap values >0.4 are shown; branches with bootstraps <0.2 were multifurcated. The scale bar at the bottom applies to 10% sequence divergence. (B) Subtree for Cryptophyceae_1 and target hits for probe Cry1–652. (C) Subtree for a part of Cercozoa_1 and target hit of probe Cerc-193 (Novel Clade 7). (D) Subtree for Katablepharidacea and target hits of probe Kat-1452. #Probe targets untrustworthy bases at the end of 18S rDNA sequences; $sequence is too short to assess potential binding of probe.

Table 1. Characteristics of CARD-FISH probes used in this study. See Fig. 2 for details in the phylogenetic positioning of the probes. The applied taxonomic terminology followed a recent review by Adl *et al.* (2019).

Probe name	Target	Coverage/outgroup hits	Sequence 5'-3'	Formamide concentration (%)	Reference
PRYM02	Haptophyta	88.6%/0	GGAATACGAGTGCCCCTGAC	30	Simon *et al.* 2000
Crypto B	Cryptophyceae_1	74.3%/1 (GU647185; Ceratium)	ACGGCCCCAACTGTCCCT	50	Metfies and Medlin 2007
Cry1–652	CRY1 lineage of cryptophytes	100%/0	TTTCACAGTWAACGATCCGCGC	30	Grujčić *et al.* 2018
Kat-1452	Uncultured Katablepharidacea	See Fig. 2: 8 sequences targeted	TTCCCGCARMATCGACGGCG	60	Grujčić *et al.* 2018
Cerc-193	Cercozoa Novel Clade 7	See Fig. 2: 1 sequence targeted	CAAGCACCGTTGCCGGATTGG	55	This study
Cerc-193-C	Competitor for probe Cerc-193		CAAGGACCGTTGCCGGATTGG		This study
Kin516	Kinetoplastea	96.2%/342 (1 Crenarchaeota, 73 SAR, 3 Diplonemea, 258 Amorphae, 7 Spermatophyta)	ACCAGACTTGTCCTCC	30	Bochdansky and Huang (2010)
EUK516	Competitor for probe Kin516	-	ACCAGACTTGCCCTCC	30	Bochdansky and Huang (2010)

in T_{50} values were determined with F-tests. To assess statistical significance of differences in the composition of HNF and ciliate assemblages among different treatments, we used one-way or two-way analysis of similarity (ANOSIM) based on Bray–Curtis distance matrices of relative proportions of protistan groups. Statistical calculations were performed in Prism 7.05 (GraphPad Software Inc.) except for ANOSIM calculated with Past 3.22 (Hammer *et al.* 2001).

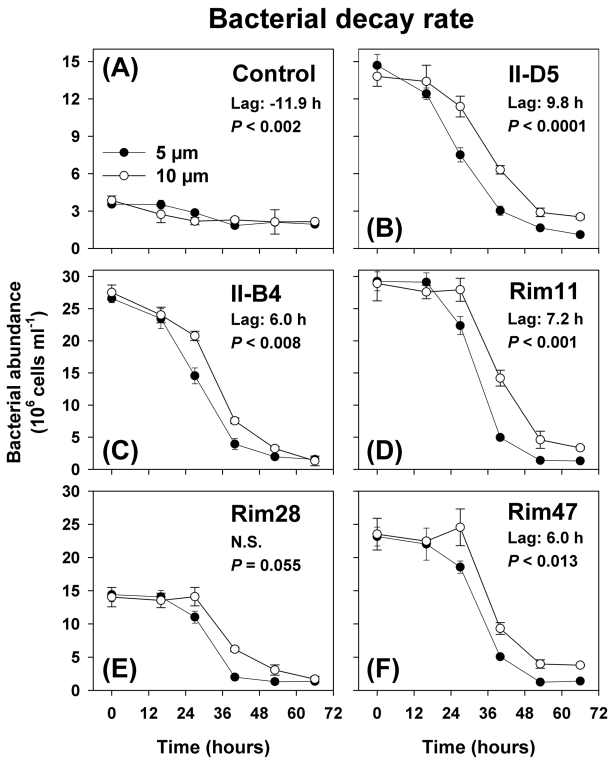

Figure 3. Time-course changes in bacterial abundance in 5- and 10-µm control treatments (**A**) with no bacteria added compared to treatments amended with five bacterial strains from the genus *Limnohabitans* (**B–F**), i.e. *L. planktonicus* (II-D5), *L. parvus* (II-B4) and undescribed strains Rim11, Rim28 and Rim47. Values are means of triplicates; error bars show SD. Decreases in bacterial abundance were significantly delayed (lag, i.e. difference in the T_{50} values, 6–9.8 h; *F*-test, $P < 0.013$–0.001) in 10-µm prey-amended treatments compared to the 5-µm ones.

RESULTS

Flagellate growth responses to bacterial prey amendments

The bacterial strains were added in different numbers (Fig. 3) yielding approximately the same initial total prey biovolume in all treatments except for the control treatments with no bacteria added. In all cases, bacterial amendments induced profound HNF growth responses (for details of growth parameters see Supplementary Fig. S1, see online supplementary material), significantly different from control treatments (from 27 to 66 h, *t*-tests with Holm-Sidak's correction for multiple comparisons, $P < 0.001$) where the HNF growth was negligible (Fig. 4). HNF abundances peaked at time points 40 or 53 h, however, in remarkable treatment-specific fashions, reflected in different amplitude and timing of the maxima and slopes of HNF increases during exponential growth phases. Consequently, also maximum growth rates (1.6–2 d^{-1}) in all but one (Rim11) 5-µm treatment, and gross growth efficiency (GGE) in all 5-µm treatments (33–40%), were significantly higher than in 10-µm treatments ($P < 0.001$, 16–32%, Supplementary Fig. S1). Moreover, the peaks in 5-µm treatments appeared sooner in II-D5, II-B4 and Rim28 (40 h) than in the corresponding 10-µm ones (53 h, Fig. 4). In contrast, HNF abundance maxima in Rim11 and Rim47 treatments were slightly delayed and occurred in parallel in both size fractions at time 53 h.

Generally, lower slopes of HNF abundance increases and time shifts in the onset of HNF growth in 10-µm treatments led to significantly longer lag phases of HNF (5.5–14 h) compared to 5-µm treatments ($P < 0.01$, Fig. 4, Supplementary Fig. S1). Moreover, lag phases in HNF growth were negligible (between 0.7 to 1.2 h) and did not differ significantly within all 5-µm treatments. Rapid bacterial decay rates (Fig. 3) without any bacterial regrowth even in control treatments led to prey depletion, commonly reflected in dramatic decreases in HNF abundances in all prey-amended treatments at the experimental endpoint (66 h, Fig. 4). However, the generally lower HNF abundances in 10-µm treatments compared to 5-µm ones, resulted in significantly delayed decreases in bacterial prey (6–9 h lag, unpaired t-test with Welch's correction, $P < 0.013$–0.001, Fig. 3) in all but one (Rim28, $P = 0.055$) 10-µm treatments.

Flagellate assemblage composition based on CARD-FISH

Our experimental manipulations resulted not only in treatment-specific time-course changes in HNF abundance, but also in significant shifts (two-way ANOSIM, $P < 0.05$) in their community composition (Figs 4 and 5). The five applied protistan probes (Fig. 2 and Table 1) cumulatively targeted 55–90% of total HNF in all but one sample (Rim47, 10-µm, 38% at 40 h; Fig. 5). Thus, the dynamics of the majority of flagellated protists could be tracked over time in high resolution (Fig. 5 and Supplementary Fig. S2, see online supplementary material).

Overall, heterotrophic Cryptophyceae (targeted by probe Crypto B) accounted for the largest fraction of HNF (35–70% of total numbers) across all treatments. All CARD-FISH-stained cells were rather small (3–5.5 µm diameter) and clearly bacterivorous with visibly ingested DAPI- and CARD-FISH-stained bacteria (Fig. 6A–C). Generally, abundances of Cryptophyceae peaked at 40 h in all treatments with bacterial amendments, reaching up to 18.8 × 10^3 cells ml^{-1} in Rim28 5-µm treatment, while they stayed relatively stable in the control treatments (1.4–2.9 × 10^3 cells ml^{-1}). These peaks, roughly coinciding with the maxima of total HNF (Figs 4 and 5), were stimulated by bacterial prey amendments. Cryptophyceae decreased in abundances at 66 h, with most striking declines in II-D5 and II-B4 10-µm treatments to numbers comparable to 0 h. They were generally more abundant in 5-µm treatments, except for Rim11, where similar numbers were recorded in both size fractions.

Within the family Cryptophyceae, the monophyletic lineage Cry1 (probe Cry1–652, Fig. 2) accounted for 15–30% of all flagellates in our experiment. CARD-FISH-stained cells were small (3–5 µm diameter) bacterivores with clearly visible bacteria in food vacuoles (Fig. 6D–F). Cry1 abundances increased in all prey-amended treatments at 40 h and decreased thereafter, except for treatments II-B4 (5-µm treatment) and Rim47 (both size fractions) where they continued to grow until the end of the experiment (Fig. 5, Supplementary Fig. S2). Moreover, Rim47 10-µm treatment showed an exceptional time-course development, i.e. the cumulative hybridization rate with all five probes dropped to only 38% of total HNF at 40 h and increased to 70 and 65% at 66 h in 5- and 10-µm Rim47 treatments, respectively. Moreover, towards the endpoint practically all Cryptophyceae were affiliated to the Cry1 lineage in the Rim47 10-µm treatment (Fig. 5, Supplementary Fig. S2) and Cry1 accounted for 6 × 10^3 cells ml^{-1} (~50% of total HNF). Consequently, absolute and relative proportions of Cry1 were significantly higher in Rim47 10-µm than in any other treatment at 66 h ($P < 0.001$, two-way ANOVA with Tukey's multiple comparisons post-tests).

Kinetoplastea (targeted by probe Kin516) showed many treatment-specific time-course changes in their relative and

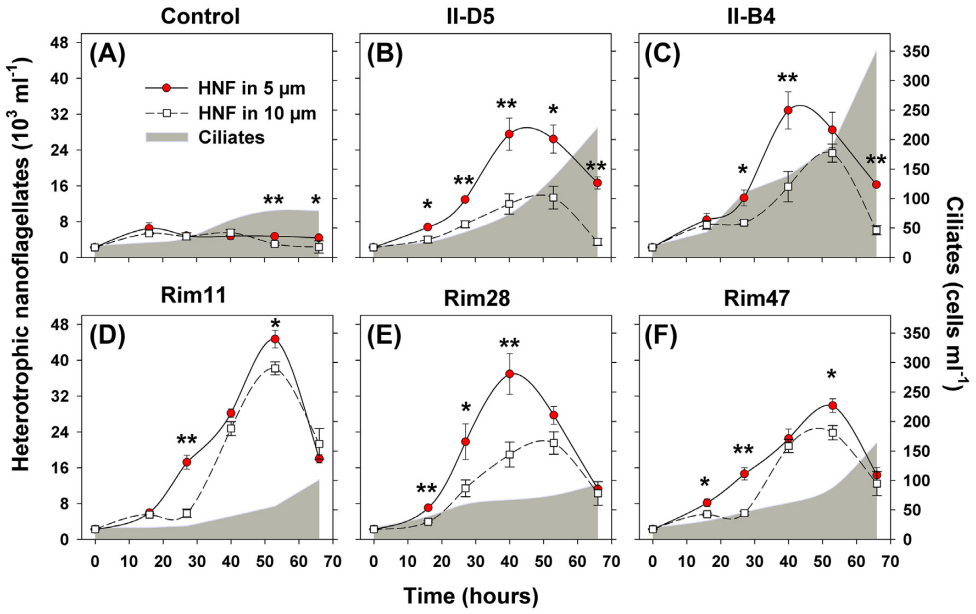

Figure 4. Time-course changes in HNF (5- and 10-µm treatments) and ciliate abundances (present only in 10-µm treatments) in control treatments with no bacteria added (**A**) compared to treatments amended with five different prey-bacteria from the genus *Limnohabitans* (for details see Fig. 1 legend and Supplementary Table S1). Asterisks above time-points indicate significantly higher flagellate abundances in 5-µm compared to the corresponding 10-µm treatments (t-tests with Holm–Sidak's correction for multiple comparisons, $^{*}P < 0.05$, $^{**}P < 0.01$). Values are means of triplicates; error bars in HNF numbers show SD.

absolute proportions (Fig. 5, Supplementary Fig. S2). These phylotypes were mostly ovoid to drop-shaped flagellates (4–7 µm length; Fig. 6G–H), with the majority of them having ingested bacteria. While Kin516 accounted for only 1.3% of total flagellates in the initial sample (0 h, corresponding to 30 cells ml^{-1}), they reached 6–10% in all 10-µm treatments, except for Rim47 (2.5%). The proportions in the latter treatments were significantly lower compared to other 10-µm treatments ($P < 0.02$). There was a general trend of higher Kin516 numbers and proportions in 10-µm treatments, with highest abundances reached in Rim11 where they were growing until the end of the experiment (1410 cells ml^{-1} and 1690 cells ml^{-1}, in 5- and 10-µm treatments, respectively).

Striking time-course changes with many treatment-specific patterns were observed for a narrow clade of Cercozoa targeted by probe Cerc-193 (compare Figs. 2, 5, and Supplementary Fig. S2). Their ovoid cells were typically 7–12 µm in size, with a large posteriorly situated nucleus and two flagella. We frequently observed well distinguishable prey cells, or at least cell remains of small HNF, yet with bright nuclei, which could be detected in food vacuoles of Cerc-193 (Fig. 6I–K). In the initial plankton sample, Cerc-193 accounted for ~3% of total HNF numbers (corresponding to 80 cells ml^{-1}), however, they showed constant growth with up to 62-fold increases in cell numbers in all prey-amended treatments while they stayed relatively stable in control treatments. The sample manipulations firstly supported rapid development of small Cryptophyceae (and its Cry1 subgroup), which was then followed by an increase of larger, predatory flagellates from the Cerc-193 lineage. Notably, this general scenario was even more obvious in 10-µm treatments. At 66 h, a highly significant increase in Cerc-193 was detected ($P < 0.001$), most marked in Rim11 and Rim28 10-µm treatments. These predatory phylotypes (Fig. 6I–K), starting from ~80 cells ml^{-1}, reached up to 600–5000 cells ml^{-1} between 40 and 66 h and their rapid increments coincided with a drastic decline in total HNF abundances, mainly in Cryptophyceae (Figs. 4, 5).

Kathablepharidae targeted by probe Kat-1452 were oblong cells with rounded ends, 7–11 µm in size, with a large posteriorly situated nucleus and two flagella. These phylotypes ingested both bacterial and HNF prey as documented by either bacteria or cell remains of flagellates visible in their food vacuoles (Fig. 6L–M). Katablepharids accounted for ~0.7% of total HNF (i.e. 20 cells ml^{-1}) at 0 h. However, our experimental setup induced rapid treatment-specific growth mainly in 10-µm treatments, with most striking peaks at 66 h (Fig. 5 and Supplementary Fig. S2). Their proportions and absolute numbers were significantly higher in the Rim11 (7.2%, 1595 cells ml^{-1}) and Rim28 (12.3%, 1346 cells ml^{-1}) than in control 10-µm treatments (2%, corresponding to 46 cells ml^{-1}; $P < 0.007$, two-way ANOVA, Tukey's post-tests). Although a slight growth stimulation of katablepharids was also recorded in 5-µm treatments, this was much less profound, with significantly lower proportions ($P < 0.03$, two-way ANOVA with Sidak's multiple comparisons post-tests) than in the corresponding 10-µm treatments, except for II-B4 (Supplementary Fig. S2).

Notably, the assumed predatory flagellates (Cerc-193 and Kat-1452, Fig. 6) reached highest relative and absolute proportions in Rim11 and Rim28 10-µm treatments (Fig. 5, Supplementary Fig. S2). Here the lowest numbers of ciliates were detected (Figs 4 and 8), which might act as competitors for prey of similar size (see below).

Flagellate lineage-specific growth rates

Cell counts with FISH-probes at times 0, 40 and 66 h allowed for tentative estimates of flagellate's lineage-specific growth rates (Fig. 7). During the first part of the experiment (0–40 h), all bacterivorous phylotypes (Crypto B, Cry1 and Kin516) showed rapid population growth corresponding to DT of 10–16 h in all 5- and 10-µm prey-amended treatments, while growth in control treatments was negligible. During the second part (40–66 h), negative population growth rates for Crypto B and Cry1 were

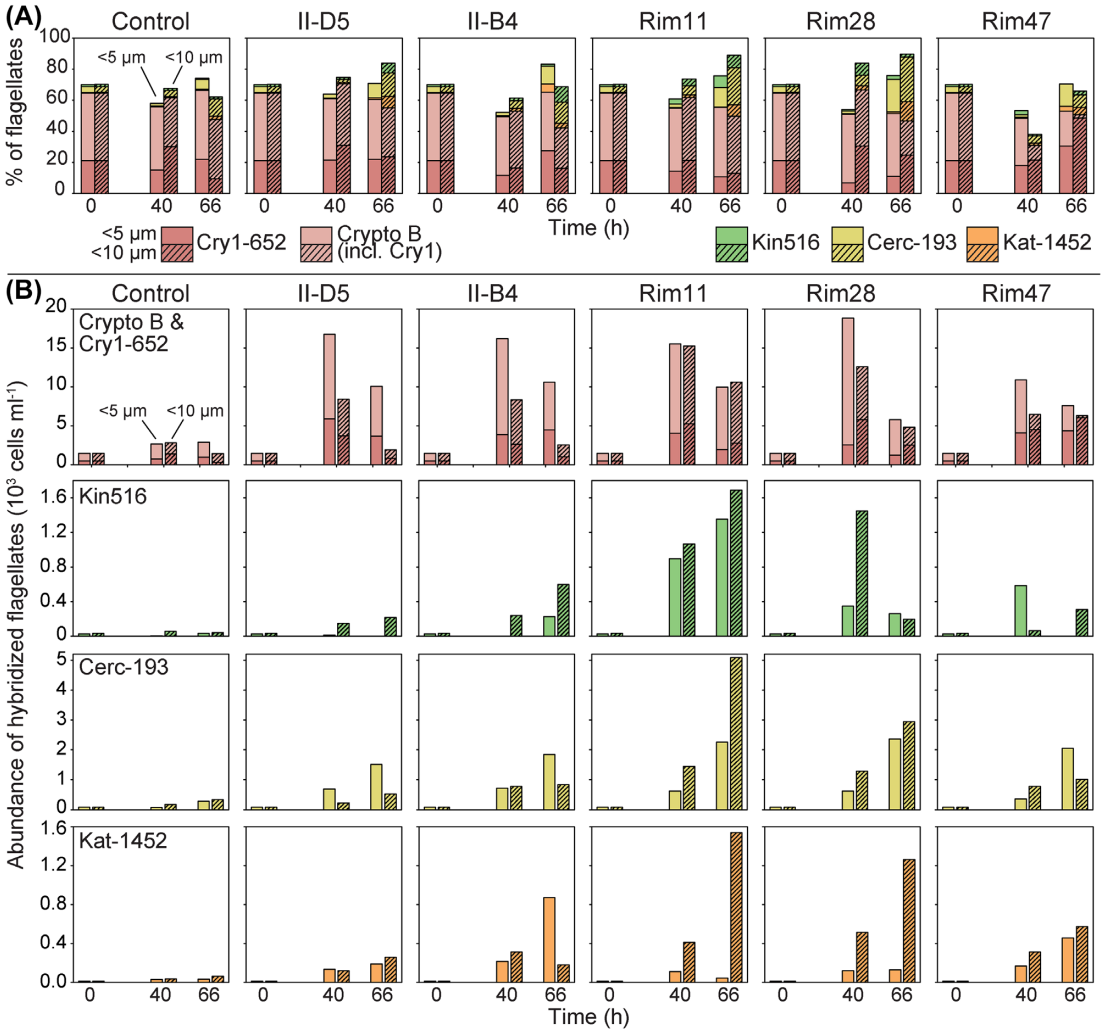

Figure 5. Relative proportions (**A**) and absolute abundances (**B**) of flagellate cells hybridized with probes targeting all Cryptophyceae (Crypto B), the Cry-1 lineage of Cryptophyceae (Cry-1, shown separately as stacked bars within total Cryptophyta, note that the total height of the column thus shows the sum of all Cryptophyta), Katablepharidacea (Kat-1452), one lineage of Cercozoa (Cerc-193), and Kinetoplastea (Kin516) in 5- and 10-µm control treatments compared to the treatments amended with five different prey-bacteria (for details see Fig. 1 legend). Time course changes in flagellate communities are compared at three different time points: 0 h, the beginning of the experiment, representing the starting community from the reservoir, with values in control treatments compared to time course changes in all treatment types; 40 and 66 h represent the proportions and abundances after 40 and 66 h of the experiment. Values are means of duplicate treatments.

observed in all prey-amended treatments as well as in the control 10-µm treatment. Kinetoplastids (Kin516) showed negative population growth only in the 5-µm prey-enriched treatments between 40 and 66 h (Fig. 7). In contrast, predatory Cercozoa and kathablepharids (Fig. 6I–M) showed consistently positive population growth throughout the whole experiment, even though total HNF abundances rapidly decreased towards the experimental endpoint (compare Figs 4 and 7). Growth dynamics corresponded to DT of ~10 h (kathablepharids) and 12–15 h (Cercozoa) between 0 and 40 h, with slower growth of kathablepharids (DT of 32–36 h) during 40–66 h.

Ciliate assemblage composition and growth

Small ciliates, as another component in 10-µm treatments, increased from ~20 cells ml^{-1} (0 h) to 94–351 cells ml^{-1} (66 h), and showed significantly higher abundances in all prey-enriched treatments than in the control (two-way ANOVA, followed by Tukey's multiple comparison post-tests, $P < 0.001$; Fig. 4). Moreover, ciliate abundances differed significantly among the prey-enriched treatments ($P < 0.001$, 66 h) reaching 351, 220 and 164 cells ml^{-1} in II-B4, II-D5 and Rim47, respectively, with treatment II-B4 being significantly different from all other variants already from 27 h till the end at 66 h ($P < 0.001$). The other two treatments, Rim11 and Rim28, showed significantly ($P < 0.001$) lower final abundances (101 and 94 cells ml^{-1}, respectively) but did not differ from each other ($P = 0.900$).

Besides the treatment-specific impacts on total ciliate abundance (Fig. 4), two-way ANOSIM indicated significant differences ($P < 0.01$) in ciliate assemblage composition. The following six major morphotype groups were detected (Fig. 8): *Urotricha* spp., *Balanion planctonicum*, *Rimostrombidium* spp., *Halteria* spp., *Cyclidium* spp. and *Cinetochilum margaritaceum*. 'Others', i.e. unidentified morphotypes, rarely accounted for >8% of total ciliates. Several general patterns of ciliate assemblage dynamics could be noted. Typical flagellate hunters, such as *Urotricha* spp. and to a lesser extent *B. planctonicum* overly dominated, whereas proportions of bacterivores such as *Cyclidium* spp. rarely exceeded 10%.

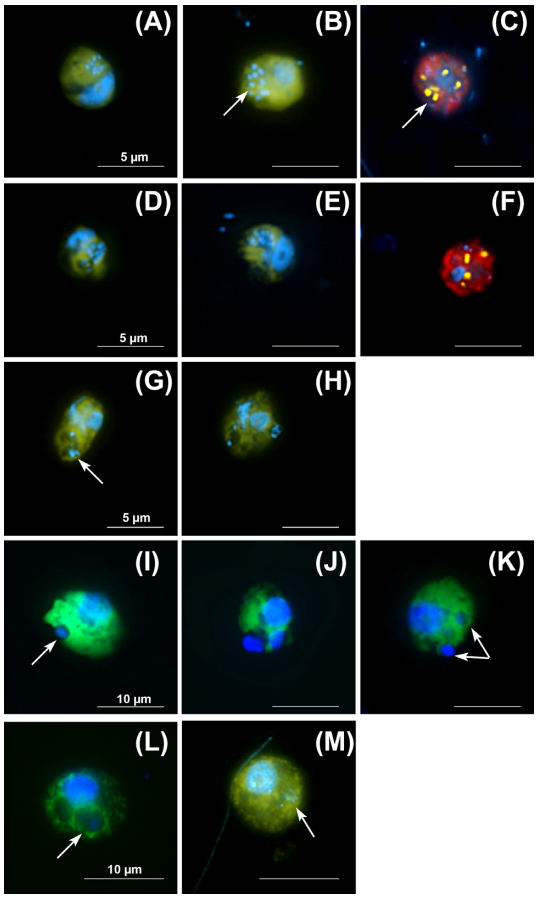

Figure 6. Microphotographs showing typical flagellate size and morphology of the cells targeted by five eukaryotic FISH probes with ingested prey from different prey-amended treatments. Shown are overlay Z-stack images of flagellates targeted by probes (FITC-stained flagellates [yellow] and DAPI-stained bacteria and flagellate nuclei [blue]; **A**, **B**, **D**, **E**, **G–M**) and of the double-hydridization of flagellates targeted by probes Crypro B or Cry1 with ingested *Limnohabitans* bacteria targeted by the R-BT065-probe (Alexa546-stained flagellates [red], DAPI-stained nuclei [blue], and fluorescein-labeled FISH-positive bacteria [yellow]; **C**, **F**). Shown are: flagellate morphotypes targeted by the Crypto B probe (A–C) and by the Cry-1 probe (D–F) with ingested bacteria; bacterivorous flagellates targeted by the probe Kin516 (**G**, **H**) with visible DAPI-stained nucleus, kinetoplast and ingested bacteria; predatory flagellates targeted by the probe Cerc-193 (**I–K**) with ingested flagellate prey or their cell remains, and targeted by the Kat-1452 probe with an ingested flagellate (**L**) or bacterial prey (**M**). White arrows highlight examples of typical positions of ingested bacteria (B, C, G, M) or flagellate prey (I, K, L) in the grazer food vacuoles. The scale bar shows length of 5 μm (A–H) and 10 μm (I–M).

Urotricha spp. was the most prominent ciliate (35–70% of total ciliates, Fig. 8), with numbers increasing towards the experimental endpoint. *Urotricha* spp. was significantly more abundant (two-way ANOVA, Tukey's post-tests, $P < 0.001$) in II-B4 (206 cells ml^{-1}) and II-D5 (148 cells ml^{-1}) than in the other treatments at 66 h, while only moderate changes in relative proportions were observed. The second most important group was represented by *Rimostrombidium* spp. (11–30% of total ciliates, 14–18 µm cell size). Abundance maxima were observed in II-B4 and II-D5 (30–59 cells ml^{-1}), while no consistent time-course patterns in relative proportions could be recorded. *Halteria* spp. declined in relative proportion over the experimental time frame, and no clear trends in the proportions of *Cyclidium* sp. and *C. margaritaceum* could be observed (Fig. 8).

DISCUSSION

Contrasting trends in abundances of bacterivorous versus predatory protists

Bacterial amendments of different size fractions of plankton stimulated profound alterations in the dynamics of diverse communities of bacterivorous (cf. Grujčić *et al.* 2018; Šimek *et al.* 2018), omnivorous or predatory flagellates (Arndt *et al.* 2000) and ciliates occurring in highly prey-specific fashions over time (Figs 4–8). The different feeding modes of major HNF players resulted in contrasting trends in population dynamics of bacterivorous versus predatory flagellates. Cryptophyceae in general and their aplastidic Cry1 lineage proliferated as long as bacterial prey was abundant (cf. Grujčić *et al.* 2018), while the largely predatory flagellate lineages Cerc-193 and Kat-1452, as well as ciliates, were over-proportionally abundant in the second phase of the experiment. These trends were clearly reflected in positive population growth of the HNF bacterivores till 40 h, followed by a decline between 40 and 66 h (Figs 5–7). In contrast, predatory HNF, benefiting from high eukaryotic prey availability, showed positive population growth also between 40 and 66 h in both 5- and 10-µm treatments. Moreover, multiple effects of an enhanced predation on smaller HNF in all 10-µm treatments were obvious from: (i) lower abundances of bacterivorous HNF resulting in decreased bulk bacterivory rates, thus delaying bacterial decay rates, (ii) lower growth rates and GGE of HNF, and (iii) longer lag phases of total HNF prior to the onset of flagellate growth compared to the corresponding 5-µm treatments (Figs 3, 4, Supplementary Fig. S1).

The enhanced predation pressure on HNF in 10-µm treatments seemed to be related to a somewhat larger inoculum of bigger predatory flagellate taxa at 0 h and the presence of ciliates, mainly of typical algivores and flagellate hunters, such as *Urotricha* spp. and *B. planctonicum* (Müller *et al.* 1991; Posch *et al.* 2015). These small prostomatid ciliates are capable of ingesting algal prey of their own size (Müller *et al.* 1991) and in our experiment showed only slightly longer DT (15–29 h) than the most rapidly growing flagellates (Fig. 7). Also the second most abundant ciliate group in our treatments, i.e. small species of *Rimostrombidium* spp. and less abundant *Halteria* spp., are considered as omnivores, ingesting food particles from bacterial size to ~8 µm large algae (Foissner, Berger and Schaumburg 1999; Posch *et al.* 2015; Šimek *et al.* 2019). Thus the vast majority of HNF morphotypes present in our experiment (Fig. 6) were within the optimal size range of major predatory protists (both flagellates and ciliates) and even filter-feeding ciliates (Jürgens and Šimek 2000; Weisse 2017; Šimek *et al.* 2019). Consequently, our initial hypothesis that bacterial enrichment will result in the dominance of fine-filter feeding bacterivorous ciliates (e.g. scuticociliates, Foissner and Berger 1996; Foissner, Berger and Schaumburg 1999) had to be rejected since raptorial ciliates clearly prevailed (Fig. 8).

Trophic cascading from bacterial prey to the grazer food chain

Interestingly, even closely related, morphologically slightly different bacteria from the genus *Limnohabitans* induced significant changes in the HNF community composition, which cascaded in highly prey-specific fashion over several trophic levels in our experiments (Figs 5–8). Thus we have gained compelling evidence that distinct taxa of planktonic bacteria may

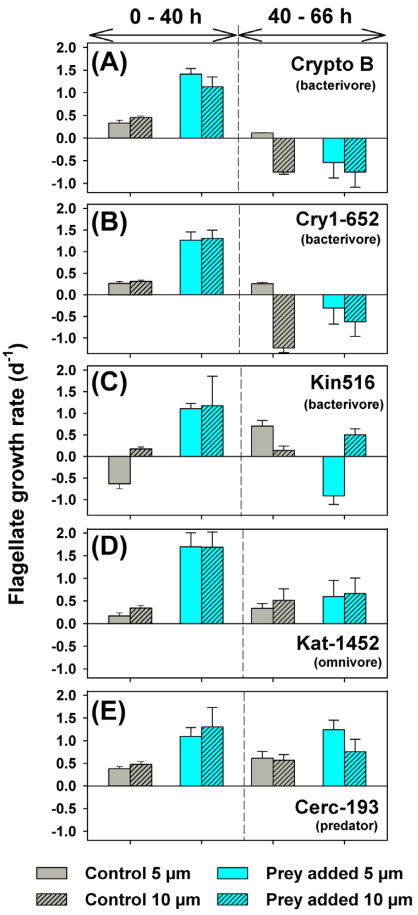

Figure 7. Flagellate lineage-specific maximum growth rates for Crypto B (**A**), Cry-1 (**B**), Kin516 (**C**), Kat-1452 (**D**) and Cerc-193 (**E**) averaged for all prey-amendments (see Fig. 1 for details of the prey types) in 5- and 10-µm treatments separately, compared to 5- and 10-µm controls. The growth rates were estimated for time intervals 0–40 h and 40–66 h. Below the probe code, the prevailing feeding mode of each flagellate group is listed in parentheses (either bacterivore, omnivore or predator, see examples in Fig. 6). Values are means of triplicates; error bars show SD.

represent food sources of different quality for primarily bacterivorous flagellate species, thus distinctly modulating the growth dynamics of certain HNF phylotypes (this study, cf. Grujčić et al. 2015, 2018; Šimek et al. 2013, 2018). Since the same initial inoculum of planktonic flagellates (5-µm) and flagellates and ciliates (10-µm) were used in the treatments, we can only speculate about additional bacterial prey-related characteristics that might induce such distinct trophic cascading effects, resulting in distinct final communities of predatory flagellates and ciliates. Thus, probably even minor differences in bacterial vulnerability or in other cellular characteristics (Boenigk and Arndt 2002; Jürgens and Matz 2002; Pernthaler 2005) might have crucial effects on the growth of some small bacterivorous flagellate taxa, which in consequence would rapidly (in hours or days) modulate the entire grazer food chain (Šimek et al. 2014, 2018).

Feeding preferences of CARD-FISH-targeted flagellates

Food vacuole analyses of CARD-FISH stained flagellates have proven to be an invaluable tool for determining feeding preferences of so far uncultivated flagellates. In our experiment, small colorless Cryptophyceae and its Cry1 lineage were identified as the most abundant bacterivorous flagellates (compare also with Piwosz *et al.* 2016; Grujčić *et al.* 2018). Another typical bacterivorous flagellate group, Kinetoplastea (Arndt *et al.* 2000; Mukherjee *et al.* 2019), had low abundances at the onset of the experiment but became markedly stimulated in several treatments, which appears to reflect their opportunistic nature (Caron 1987; Boenigk and Arndt 2000). Their low abundances in the initial sample, taken from the surface layer of the reservoir, corresponded well with findings that kinetoplastids feed mainly on particle-associated bacteria and dominated the HNF communities in deep strata of freshwater lakes (Arndt *et al.* 2000; Mukherjee, Hodoki and Nakano 2015; Mukherjee *et al.* 2019). For other typical bacterivorous flagellate groups such as choanoflagellates (distinguishable by the presence of a collar), and chrysophytes (Arndt *et al.* 2000; Jürgens and Matz 2002) we do not have FISH-probes and thus we cannot provide quantitative estimates of their contributions to the flagellate community in different treatments. This somehow limits the possibility of generalizing our data on the role of different flagellate groups as bacterivores. On the other hand, our recent results from three different reservoirs and four fishponds, representing a total of 60 samples (Šimek and Mukherjee, unpublished data), showed that aplastidic bacterivorous Cryptophyceae and its Cry1 lineage accounted, on average, for 40–60% and 15–40% of total HNF, respectively.

CARD-FISH probes Cerc-193 and Kat-1452 (targeting a cercozoan clade and katablepharids, respectively) revealed the most important predatory flagellates in our experiment, and inspecting their food vacuole contents provided qualitative evidence for their prevailing feeding mode (Fig. 6). Overall, these predatory flagellate groups capable of preying upon small HNF reached up to 2–5 $\times$ 10^3 cells ml^{-1} in many treatments at 66 h (Fig. 5). Many of them contained cell remains of HNF or at least clearly visible nuclei of ingested HNF, yet quantifications of individual uptake rates of small flagellates by the predatory phylotypes was not possible. Our study is likely among the first trying to unveil the role of selected freshwater pelagic predatory Cercozoa (compare Hess and Melkonian 2013) and katablepharids under close to *in situ* conditions. Katablepharidacea are known to prey on larger prey such as different algae (Clay and Kugrens 1999; Ok *et al.* 2018) with a peculiar way of feeding by forming swarms, as observed in some cultures (Clay and Kugrens 1999; Okamoto and Inouye 2005). Recently, the free-living species *Katablepharis japonica* has been reported to feed on red-tide forming algae (Kwon *et al.* 2017). Interestingly, Katablepharidacea targeted by probe Kat-1452 contained concurrently bacteria (compare Domaizon *et al.* 2003) and small HNF in their food vacuoles in our study, ranking them as omnivorous or predatory flagellates.

Notably, the narrow Cerc-193 clade was entirely dominated by predatory cells. They formed a considerable part of the total HNF community at the end of our experiment (up to 24–28%), either due to attenuated grazing losses or potential removal of their competitors. Similar dynamics for the same Cercozoan phylotype has been found in other manipulation experiments with a comparable setup (Mehrshad and coauthors, unpublished data). For designing the probe Cerc-193, metagenomic and amplicon 18S rRNA gene sequences retrieved from these experiments were used, including the only publicly available sequence for these Cercozoa affiliated with Novel Clade 7 (Bass and Cavalier-Smith 2004). By translating the Cerc-193 proportions to absolute numbers, they frequently comprised 2–5 $\times$ 10^3 cells ml^{-1}, i.e. they were generally by one order of magnitude

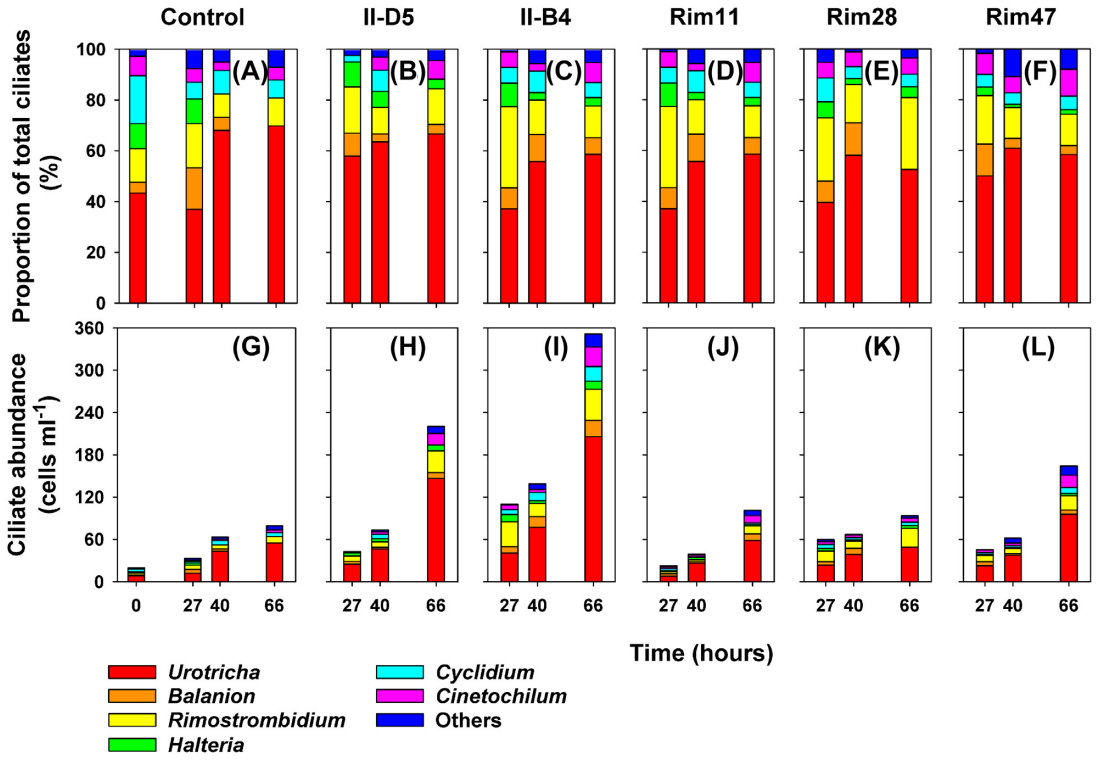

Figure 8. Relative proportions (**A–F**) and absolute abundances of ciliates cells (**G–L**) in 10-μm treatments representing the following six major morphotype groups: *Urotricha* spp., *Balanion planctonicum*, *Rimostrombidium* spp., *Halteria* sp., *Cyclidium* sp. and *Cinetochilum margaritaceum*. The seventh ciliate group 'Others' represents unidentified morphotypes or very rarely observed species. Values are means of triplicate treatment.

more abundant than the typical raptorial ciliates *Urotricha* spp. and *B. planctonicum* (Müller *et al.* 1991; Posch *et al.* 2015).

As no live observations of food uptake were possible and no pure culture of the Cerc-193 phylotype was available, we had to rely solely on CARD-FISH preparations. We frequently observed partial or complete engulfment of smaller HNF prey by pseudopodia projected from the edges of these obligate predators, which had usually 1–4 food vacuoles containing flagellate remains at different degrees of digestion (Fig. 6I–K). Moreover, our observations allow for tentative estimates of prey consumption rates by these Cercozoa: Bacterivorous cryptophytes had a median cell diameter of 4.2 μm and predatory Cerc-193 had a diameter of ~9 μm, corresponding to cell volumes of 39 and 382 μm^3, respectively. Thus, biovolumes of prey and predator differed by approximately one order of magnitude. As the predator grew with a DT of 10–20 h and by assuming a GGE of 29% (Šimek *et al.* 2018), these predators had to graze ~35 small flagellates to meet their carbon requirements per one doubling. These data speak for the remarkable total grazing impact of the predatory flagellates occurring in densities of 10^3 ml^{-1}, which was also reflected in the negative population development of small bacterivorous cryptophytes towards the experimental endpoint (Figs. 5–7). Thus, the two rapidly growing predatory (Cerc-193) or omnivorous (Kat-1452) flagellate groups were likely the core grazers of small bacterivorous HNF groups in our experiment. However, predatory prostome ciliates and omnivorous *Rimostrombidium* spp. also significantly contributed to HNF mortality in our experiment, which is in line with literature reports suggesting ciliates as efficient HNF grazers in lakes (Nakano *et al.* 2001; Weisse *et al.* 2016).

Unveiling ecological traits of uncultured protistan taxa

While our data provided compelling evidence on the prevailing feeding modes of the FISH-targeted flagellate groups in our treatments (Fig. 6), we have only a limited and rather mosaic knowledge about the ecological functions of these highly diverse flagellates. Essential parts of bacterivorous and omnivorous protistan taxa are largely known and their role in aquatic food webs is well studied (Arndt *et al.* 2000; Montagnes *et al.* 2008; Weisse 2017; Šimek et al. 2018, 2019), however, predatory cercozoans in marine (Berney *et al.* 2013), brackish (Piwosz and Pernthaler 2011) and freshwater ecosystems are still understudied. Moreover, ~10–45% of total HNF were not targeted by any of the applied CARD-FISH-probes in our study, thus we are missing data on the feeding ecology of a considerable proportion of flagellate taxa present.

Predatory flagellates might be present in rather low abundances in natural plankton due to strong exploitative competition between protistan predators and severe top-down control by larger zooplankton (Arndt *et al.* 2000; Jürgens and Jeppesen 2000; Sommer *et al.* 2012). For instance, the larger cercozoans and katablepharids (Cerc-193 and Kat-1452) accounted initially only for 3–4% and 1–2% of total HNF in the natural community, respectively (Fig. 5, cf. Grujčić *et al.* 2018; Mehrshad and coauthors, unpublished data). However, their proportions increased to 24–28% and 7–12% of total HNF, respectively, when experimental manipulations stopped the top-down control of HNF. We are aware that experimental workflows create disturbances of established interactions between major microbial players, as treatments usually tend to simplify complex food webs by reducing the degree of trophic levels (Jürgens and Jeppesen 2000;

Šimek *et al.* 2018). Thus, manipulated communities experience faster and stronger changes with an overexploitation of certain vulnerable and less resilient members, as distinct predators are not under top-down control. However, exactly this aspect can become a powerful tool for an enrichment of otherwise less abundant protistan taxa that might play an important role in the carbon flow to higher trophic levels. This reiterates the advantage of experimental manipulations in disentangling food webs interactions (Jürgens and Jeppesen 2000; Šimek et al. 2013, 2018) to elucidate the trophic mode of environmentally relevant but less abundant flagellate taxa (Fig. 6, cf. Simon *et al.* 2015; Grujčić *et al.* 2018).

Moreover, recent progress in sequencing allows for targeting more planktonic protists by newly designed FISH-probes (Massana *et al.* 2009; Piwosz *et al.* 2016; Grujčić *et al.* 2018, this study) even if cultivation-based approaches fail. FISH-probes facilitate the visualization of important flagellate taxa *in situ* and the inspection of their food vacuole contents provides at least qualitative evidence of their feeding modes. Moreover, FISH-probes are needed for a reliable quantification of flagellate taxa, which is not possible with application of sequencing methods only (Piwosz *et al.* 2020). Thus, we suggest experimental manipulation in combination with the design of novel FISH-probes as relevant approaches in addition to cultivation-based studies. This workflow is powerful enough to provide valuable insights into the life strategies of so far unknown or morphologically indistinguishable protists and to elucidate yet unknown trophic interactions of uncultured protists that form highly complex microbial food webs.

SUPPLEMENTARY DATA

Supplementary data are available at FEMSEC online.

ACKNOWLEDGMENT

We thank R. Malá and M. Štojdlová for their excellent laboratory assistance and P. Znachor for editing of the micrographs.

FUNDING

The study was supported by the European Union within ESIF in frame of Operational Programme Research, Development and Education (project no. CZ.02.1.01/0.0/0.0/16_025/0007417). Additional support was provided by the CSF grant 13-00243S awarded to K.Š. and by 19-23469S and 20-12496X awarded to M.M.S.

Conflict of Interest. None declared.

REFERENCES

Adl SM, Bass D, Lane CE *et al.* Revisions to the classification, nomenclature, and diversity of eukaryotes. *J Euk Microbiol* 2019;**66**:4–119.

Arndt H, Dietrich D, Auere B *et al.* Functional diversity of heterotrophic flagellates in aquatic ecosystems. In: Leadbeater BSC, Green JC . (eds.). *The Flagellates*. London Taylor and Francis, 2000, 240–68.

Bass D, Cavalier-Smith T. Phylum-specific environmental DNA analysis reveals remarkably high global biodiversity of Cercozoa (Protozoa). *Int J Syst Evol Micr* 2004;**54**:2393–404.

Beisner BE, Grossart H-P, Gasol JM. A guide to methods for estimating phago-mixotrophy in nanophytoplankton. *J Plankton Res* 2019;**41**:77–89.

Berney C, Romac S, Mahe F *et al.* Vampires in the oceans: predatory cercozoan amoebae in marine habitats. *ISME J* 2013;**7**:2387–99.

Berninger UB, Finlay J, Kuuppo-Leinikki P. Protozoan control of bacterial abundances in freshwaters. *Limnol Oceanogr* 1991;**36**:139–47.

Bochdanksy AB, Huang L. Re-evaluation of the EUK516 probe for the domain eukarya results in a suitable probe for the detection of Kinetoplastids, an important group of parasitic and free-living flagellates. *J Eukaryot Microbiol* 2010;**57**: 229–35.

Boenigk J, Arndt H. Bacterivory by heterotrophic flagellates: community structure and feeding strategies. *Antonie Van Leeuwenhoek* 2002;**81**:465–80.

Boenigk J, Arndt H. Particle handling during interception feeding by four species of heterotrophic nanoflagellates. *J Eukaryot Microbiol* 2000;**47**:350–58.

Caron DA. Grazing of attached bacteria by heterotrophic microflagellates. *Microb Ecol* 1987;**13**:203–18.

Clay B, Kugrens P. Systematics of the enigmatic kathablepharids, including EM characterization of the type species, *Kathablepharis phoenikoston*, and new observations on *K. remigera* comb. nov. *Protist* 1999;**150**:43–59.

Domaizon I, Viboud S, Fontvieille D. Taxon-specific and seasonal variations in flagellates grazing on heterotrophic bacteria in the oligotrophic Lake Annecy - importance of mixotrophy. *FEMS Microbiol Ecol* 2003;**46**:317–29.

Foissner W, Berger H, Schaumburg J. Identification and ecology of limnetic plankton ciliates. *Informationsberichte des Bayer Landesamtes für Wasserwirtschaft Heft* 3/99, 1999;**793**.

Foissner W, Berger H. A user-friendly guide to the ciliates (Protozoa, Ciliophora) commonly used by hydrobiologists as bioindicators in rivers, lakes, and waste waters, with notes on their ecology. *Freshw Biol* 1996;**35**:375–482.

Grujčić V, Kasalický V, Šimek K. Prey-specific growth responses of freshwater flagellate communities induced by morphologically distinct bacteria from the genus *Limnohabitans*. *Appl Environ Microbiol* 2015;**81**:4993–5002.

Grujčić V, Nuy J, Salcher MM *et al.* Cryptophyta as major freshwater bacterivores in experiments with manipulated bacterial prey. *ISME J* 2018;**12**:1668–81.

Hahn MW, Stadler P, Wu QL *et al.* The filtration acclimatization method for isolation of an important fraction of the not readily cultivable bacteria. *J Microbiol Methods* 2004;**57**:379–90.

Hammer Ø, Harper DAT, Ryan PD. Past: Paleontological Statistics Software Package for Education and Data Analysis. *Palaeontol Electron* 2001;**4**:art.4.

Havskum H, Riemann B. Ecological importance of bacterivorous, pigmented flagellates (mixotrophs) in the Bay of Aarhus, Denmark. *Mar Ecol Prog Ser* 1996;**137**:251–63.

Hess S, Melkonian M. The Mystery of clade X: *Orciraptor* gen. nov. and *Viridiraptor* gen. nov. are highly specialised, algivorous Amoeboflagellates (Glissomonadida, Cercozoa). *Protists* 2013;**164**:706–47.

Jeuck A, Arndt H. A short guide to common heterotrophic flagellates of freshwater habitats based on the morphology of living organisms. *Protist* 2013;**164**:842–60.

Jezbera J, Horňák K, Šimek K. Food selection by bacterivorous protists: Insight from the analysis of the food vacuole content by means of fluorescence in situ hybridization. *FEMS Microbiol Ecol* 2005;**52**:351–63.

Jürgens K, Jeppesen E. The impact of metazooplankton on the structure of the microbial food web in a shallow, hypertrophic lake. *J Plankton Res* 2000;**22**:1047–70.

Jürgens K, Matz C. Predation as a shaping force for the phenotypic and genotypic composition of planktonic bacteria. *Antonie Van Leeuwenhoek* 2002;**81**:413–34.

Jürgens K, Šimek K. Functional response and particle size selection of *Halteria* cf. *grandinella*, a common freshwater oligotrichous ciliate. *Aquat Microb Ecol* 2000;**22**:57–68.

Kasalický V, Jezbera J, Šimek K *et al.* The diversity of the *Limnohabitans* genus, an important group of freshwater bacterioplankton, by characterization of 35 isolated strains. *PLoS One* 2013;**8**:e58209.

Kiørboe T. How zooplankton feed: mechanisms, traits and trade-offs. *Biol Rev* 2011;**86**:311–39.

Kwon JE, Jeong HJ, Kim SJ *et al.* Newly discovered role of the heterotrophic nanoflagellate *Katablepharis japonica*, a predator of toxic or harmful dinoflagellates and raphidophytes. *Harmful Algae* 2017;**68**:224–39.

Ludwig W, Strunk O, Westram R *et al.* ARB: a software environment for sequence data. *Nucl Acid Res* 2004;**32**:1363–71.

Massana R, Unrein F, Rodríguez-Martínez R *et al.* Grazing rates and functional diversity of uncultured heterotrophic flagellates. *ISME J* 2009;**3**:588–96.

Metfies K, Medlin LK. Refining cryptophyte identification with DNA-microarrays. *J Plankton Res* 2007;**29**:1071–75.

Montagnes DJS, Barbosa AB, Boenigk J *et al.* Selective feeding behaviour of key free-living protists: avenues for continued study. *Aquat Microb Ecol* 2008;**53**:83–98.

Mukherjee I, Hodoki Y, Nakano S. Kinetoplastid flagellates overlooked by universal primers dominate in the oxygenated hypolimnion of Lake Biwa, Japan. *FEMS Microbiol Ecol* 2015;**91**:1–11.

Mukherjee I, Hodoki Y, Okazaki Y *et al.* Widespread dominance of kinetoplastids and unexpected presence of diplonemids in deep freshwater lakes. *Front Microbiol* 2019;**10**:2375.

Müller H, Schöne A, Pinto-Coelho RM *et al.* Seasonal succession of ciliates in Lake Constance. *Microb Ecol* 1991;**21**:119–38.

Nakano S, Ishii N, Manage PM *et al.* Trophic roles of heterotrophic nanoflagellates and ciliates among planktonic organisms in a hypereutrophic pond. *Aquat Microb Ecol* 2001;**16**:153–61.

Okamoto N, Inouye I. The katablepharids are a distant sister group of the Cryptophyta: A proposal for Katablepharidophyta divisio nova/Kathablepharida phylum novum based on SSU rDNA and beta-tubulin phylogeny. *Protist* 2005;**156**:163–79.

Ok JH, Jeong HJ, Lim AS *et al.* Feeding by the heterotrophic nanoflagellate *Katablepharis remigera* on algal prey and its nationwide distribution in Korea. *Harmful Algae* 2018;**74**: 30–45.

Pernthaler J. Predation on prokaryotes in the water column and its ecological implications. *Nat Rev Microbiol* 2005;**3**:537–46.

Piwosz K, Kownacka J, Ameryk A *et al.* Phenology of cryptomonads and the CRY1 lineage in a coastal brackish lagoon (Vistula Lagoon, Baltic Sea). *J Phycol* 2016;**53**:1689–99.

Piwosz K, Pernthaler J. Enrichment of omnivorous Cercozoan nanoflagellates from coastal Baltic Sea waters. *PLoS One* 2011;**6**:e24415.

Piwosz K, Pernthaler J. Seasonal population dynamics and trophic role of planktonic nanoflagellates in coastal surface waters of the Southern Baltic Sea. *Environ Microbiol* 2010;**12**:364–77.

Piwosz K, Shabarova T, Pernthaler J *et al.* Bacterial and eukaryotic small-subunit amplicon data do not provide a quantitative picture of microbial communities, but are they reliable in the context of their ecological interpretation. *mSphere* 2020;**5**:e00052–20.

Piwosz K. Weekly dynamics of abundance and size structure of specific nanophytoplankton lineages in coastal waters (Baltic Sea). *Limnol Oceanogr* 2019;**64**:2172–86.

Posch T, Eugster B, Pomati F *et al.* Network of interactions between ciliates and phytoplankton during spring. *Front Microbiol* 2015;**6**:1286.

Quast C, Pruesse E, Yilmaz P *et al.* The SILVA ribosomal RNA gene database project: improved data processing and web-based tools. *Nucl Acid Res* 2013;**41**:D590–6.

Sekar RA, Pernthaler J, Pernthaler F *et al.* An improved protocol for quantification of freshwater Actinobacteria by fluorescence in situ hybridization. *Appl Environ Microbiol* 2003;**69**:2928–35.

Sherr BF, Sherr EB, Fallon RD. Use of monodispersed fluorescently labeled bacteria to estimate in situ protozoan bacterivory. *Appl Environ Microbiol* 1987;**53**:958–65.

Simon M, López-García P, Deschamps P *et al.* Marked seasonality and high spatial variability of protist communities in shallow freshwater systems. *ISME J* 2015;**9**:1–13.

Simon N, Campbell L, Ornolfsdottir E *et al.* Oligonucleotide probes for the identification of three algal groups by dot blot and fluorescent whole-cell hybridization. *J Eukaryotic Microbiol* 2000;**47**:76–84.

Sommer U, Adrian R, De Senerpont Domis L *et al.* Beyond the Plankton Ecology Group (PEG) Model: Mechanisms driving plankton succession. *Annu Rev Ecol Evol Syst* 2012;**43**:429–48.

Stamatakis A. RAxML version 8: a tool for phylogenetic analysis and post-analysis of large phylogenies. *Bioinformatics* 2014;**30**:1312–13.

Šimek K, Grujčić V, Hahn MW *et al.* Bacterial prey food characteristics modulate community growth response of freshwater bacterivorous flagellates. *Limnol Oceanogr* 2018;**63**:484–502.

Šimek K, Grujčić V, Nedoma J *et al.* Microbial food webs in hypertrophic fishponds: omnivorous ciliate taxa are major protistan bacterivores. *Limnol Oceanogr* 2019;**64**:2295–309.

Šimek K, Kasalický V, Jezbera J *et al.* Differential freshwater flagellate community response to bacterial food quality with a focus on *Limnohabitans* bacteria. *ISME J* 2013;**7**:1519–30.

Šimek K, Nedoma J, Znachor P *et al.* A finely tuned symphony of factors modulates the microbial food web of a freshwater reservoir in spring. *Limnol Oceanogr* 2014;**59**:1477–92.

Šimek K, Pernthaler J, Weinbauer MG *et al.* Changes in bacterial community composition, dynamics and viral mortality rates associated with enhanced flagellate grazing in a meso-eutrophic reservoir. *Appl Environ Microbiol* 2001;**67**: 2723–33.

Unrein F, Gasol JM, Not F *et al.* Mixotrophic haptophytes are key bacterial grazers in oligotrophic coastal waters. *ISME J* 2014;**8**:164–76

Weisse T, Anderson R, Arndt H *et al.* Functional ecology of aquatic phagotrophic protists – concepts, limitations, and perspectives. *Eur J Protisto1* 2016;**55**:50–74.

Weisse T. Functional diversity of aquatic ciliates. *Europ J Protistol* 2017;**61**:331–58.

Yilmaz LS, Parnerkar S, Noguera DR. MathFISH, a web tool that uses thermodynamics-based mathematical models for in silico evaluation of oligonucleotide probes for fluorescence *in situ* hybridization. *Appl Environ Microbiol* 2011;**77**:1118–22.